

Functionalization and Capping of a CdS Nanocluster: A Study of Ligand Exchange by Electrospray Mass Spectrometry

Thomas Løver,[†] William Henderson,[‡] Graham A. Bowmaker,^{*,†}
John M. Seakins,[†] and Ralph P. Cooney[†]

Department of Chemistry, University of Auckland, Private Bag 92019,
Auckland, New Zealand, and Department of Chemistry, University of Waikato,
Private Bag 3105, Hamilton, New Zealand

Received March 13, 1997. Revised Manuscript Received June 16, 1997[⊗]

Electrospray mass spectrometry is a powerful technique for investigating the capping and the functionalization of the surface of a CdS nanocluster, via ligand-exchange reactions. The reactions of the thiophenolate-capped CdS cluster $[S_4Cd_{17}(SPh)_{28}]^{2-}$ with thiols (HSR), dithiols (HSRSH), thiol acids (HSRCOOH), thio acids (RCOSH), thiol alcohols (HORSH), diethyldithiocarbamate $[Et_2NCSS]^-$, isopropylxanthate $[(CH_3)_2CHOCSS]^-$ and 3-mercaptopropyltrimethoxysilane $[HS(CH_2)_3Si(OCH_3)_3]$ have been investigated. Information about the extent of exchange, bonding modes and cluster transformations is obtained. Almost complete exchange was observed for *p*-toluenethiol while the exchange with *o*-toluenethiol and 1-dodecanethiol was restricted owing to steric hindrance. The thiol acids HSRCOOH bind as the doubly charged $[R(S)COO]^{2-}$ ligand, chelating to neighboring cadmium atoms through both the thiol group and one of the oxygen atoms of the carboxylic acid group. The exchange with the thio acids $[RCOSH]$ involves terminal $[RCOS]^-$ ions. Diethyldithiocarbamate $[(C_2H_5)_2NCSS]^-$ and isopropylxanthate $[(CH_3)_2CHOCSS]^-$ remove cadmium atoms from the surface of the cluster due to the formation of terminal S,S-chelating bonds. 3-Mercaptopropyltrimethoxysilane $HS(CH_2)_3Si(OCH_3)_3$ readily exchanged to yield the silane-functionalized clusters $[S_4Cd_{17}(SPh)_{28-n}\{S(CH_2)_3Si(OCH_3)_3\}_n]^{2-}$ ($n = 1-11$).

Introduction

Semiconductor nanoclusters are currently under intense investigation in various fields of science.¹⁻⁵ Quantum size effects result in unique physical and chemical properties that depend strongly on the size of the cluster.^{6,7} Advanced materials built up from nanoscale particles give promise of a wide range of innovative applications in catalysis, sensors, nonlinear optics and molecular electronics.⁸⁻¹⁰ Methods that permit uniform clusters to be prepared are necessary to study and control the properties of nanocluster materials. Significant progress has been made, particularly in the preparation of group II–VI semiconductors, by using capping ligands, such as thiolates, which cap the particle surface by direct coordination to surface atoms. The process typically involves precipitation of the semiconductor material in the presence of the capping species¹¹⁻¹⁹ or growth of larger clusters from molecular precursors

which already incorporate the capping ligands.²⁰⁻²² Combined recently with size-selective precipitation,^{11,15} this technique allows fully redispersible powders of materials with narrow size distributions (<5% in diameter) to be obtained. The synthesis of some clusters with well-defined structures has also been achieved. These include the thiophenolate-capped clusters $[EM_8(SPh)_{16}-(Me_4N)_2]$,²³ $[E_4M_{10}(SPh)_{16}](Me_4N)_4$ ($M = Cd, Zn; E = Se, S$),²⁴ $[S_4Cd_{17}(SPh)_{28}](Me_4N)_2$,²⁵ $[S_4Cd_{17}(SCH_2CH(OH)CH_3)_{26}]$,²⁶ $[S_{14}Cd_{32}(SPh)_{36} \cdot 4DMF]$,²¹ and $[S_{14}Cd_{32}(SCH_2CH(OH)CH_3)_{36} \cdot 4H_2O]$.¹⁵

[†] University of Auckland.

[‡] University of Waikato.

[⊗] Abstract published in *Advance ACS Abstracts*, August 1, 1997.

- (1) Alivisatos, A. P. *Science* **1996**, *271*, 933–937.
- (2) Steigerwald, M. L.; Brus, L. E. *Acc. Chem. Res.* **1990**, *23*, 183–188.
- (3) Weller, H. *Angew. Chem., Int. Ed. Engl.* **1993**, *32*, 41–53.
- (4) Henglein, A. *Chem. Rev.* **1989**, *89*, 1861–1873.
- (5) Wang, Y.; Herron, N. *J. Phys. Chem.* **1991**, *95*, 525–532.
- (6) Weller, H. *Angew. Chem., Int. Ed. Engl.* **1993**, *32*, 41–53.
- (7) Vossmeier, T.; Katsikas, L.; Giersig, M.; Popovic, I. G.; Diesner, K.; Chemseddine, A.; Eychmüller, A.; Weller, H. *J. Phys. Chem.* **1994**, *98*, 7665–7673.
- (8) Wen, J.; Wilkes, G. L. *Chem. Mater.* **1996**, *8*, 1667–1681.
- (9) Schubert, U. *J. Chem. Soc., Dalton Trans.* **1996**, 3343–3348.
- (10) Schubert, U.; Tewinkel, S.; Lamber, R. *Chem. Mater.* **1996**, *8*, 2047–2055.

(11) Murray, C. B.; Norris, D. J.; Bawendi, M. G. *J. Am. Chem. Soc.* **1993**, *115*, 8706–8715.

(12) Noglik, H.; Pietro, W. J. *Chem. Mater.* **1994**, *6*, 1593–1595.

(13) Nosaka, Y.; Shigeno, H.; Ikeuchi, T. *J. Phys. Chem.* **1995**, *99*, 8317–8322.

(14) Hayes, D.; Micic, O. I.; Nenadovic, M. T.; Swayambunathan V.; Meisel, D. *J. Phys. Chem.* **1989**, *93*, 4603–4608.

(15) Vossmeier, T.; Reck, G.; Schulz, B.; Katsikas, L.; Weller, H. *J. Am. Chem. Soc.* **1995**, *117*, 12881–12882.

(16) Marcus, M. A.; Flood, W.; Stiegerwald, M.; Brus, L.; Bawendi, M. *J. Phys. Chem.* **1991**, *95*, 1572–1576.

(17) Kortan, A. R.; Hull, R.; Opila, R. L.; Bawendi, M. G.; Steigerwald, M. L.; Carrol, P. J.; Brus, L. E. *J. Am. Chem. Soc.* **1990**, *112*, 1327–1332.

(18) Steigerwald, M. L.; Alivisatos, A. P.; Gibson, J. M.; Harris, T. D.; Kortan, R.; Muller, A. J.; Thayer, A. M.; Duncan, T. M.; Douglass, D. C.; Brus, L. E. *J. Am. Chem. Soc.* **1988**, *110*, 3046–3050.

(19) Herron, N.; Wang, Y.; Eckert, H. *J. Am. Chem. Soc.* **1990**, *112*, 1322–1326.

(20) Herron, N.; Suna, A.; Wang, Y. *J. Chem. Soc., Dalton Trans.* **1992**, 2329–2335.

(21) Herron, N.; Calabrese, J. C.; Farneth, W. E.; Wang, Y. *Science* **1993**, *259*, 1426–1428.

(22) Løver, T.; Bowmaker, G. A.; Seakins, J. M.; Cooney, R. P.; Henderson, W. *J. Mater. Chem.*, **1997**, *7*, 647–651.

(23) Lee, G. S. H.; Fisher, K. J.; Craig, D. C.; Scudder, M. L.; Dance, I. G. *J. Am. Chem. Soc.* **1990**, *112*, 6435–6437.

Recent developments suggest that future research will be directed toward the controlled and rational design of nanometer-scale assemblies (two- and three-dimensional superlattices) and of nanocomposites, bulk materials built from nanometer constituents. A key role in this is the development of the chemistry of capping and functionalizing ligands. An example is the achievement of a three-dimensional CdSe quantum dot superlattice reported by Bawendi and co-workers.²⁷ These superlattices exhibit collective bulk properties, which emerge from the ordered array of their constituents. The collective properties can be controlled by adjusting the distance between the individual nanoparticles by varying the size of the ligands that cap the surface of the clusters. Bifunctional capping ligands can be used to aid dispersion of the clusters in a host such as an oxide, polymer or to form layered nanostructures.^{28,29} A recent example is the synthesis of Au particles coated with a layer of silica using the bifunctional ligand (3-amino-propyl)trimethoxysilane ($\text{NH}_2(\text{CH}_2)_3\text{Si}(\text{OCH}_3)_3$) as a coupler.²⁹ The preparation of similar systems of group II–VI semiconductors and metal oxides may result from the use of thiolate ions, SR^- , carrying a functional group which can chelate to the metals of metal alkoxides. The metal alkoxides $\text{M}(\text{OR})_x$ (M = metal of valency x , R = alkyl or aryl group) form metal oxides by hydrolysis, the so-called “sol–gel process”. Functional groups which complex with metal alkoxides are carboxylic acids, alcohols, amino acids, β -diketones, and β -ketoesters.³⁰ Developments in the use of these bifunctional ligands, which are capable of connecting non-oxides with metal oxides, are expected to provide further opportunities in sol–gel prepared optical solids based on dispersed inorganic nanoparticles.

In this paper we present a uniquely suited method for the study of the reaction of various ligand types with a well-defined CdS nanocluster. Recently we have demonstrated that electrospray mass spectrometry (ESMS) is a powerful technique for characterizing thiolate-capped metal chalcogenide clusters.^{31,32} This relatively new technique allows ions to be transferred from solution to the gas phase, followed by conventional mass analysis.^{33,34} The electrospray ionization process is soft and results in minimal fragmentation of the cluster ions, thus allowing the detection of solution species. The technique is particularly suited for the study of metal-ion and ligand-exchange processes and has been compared with low-temperature NMR

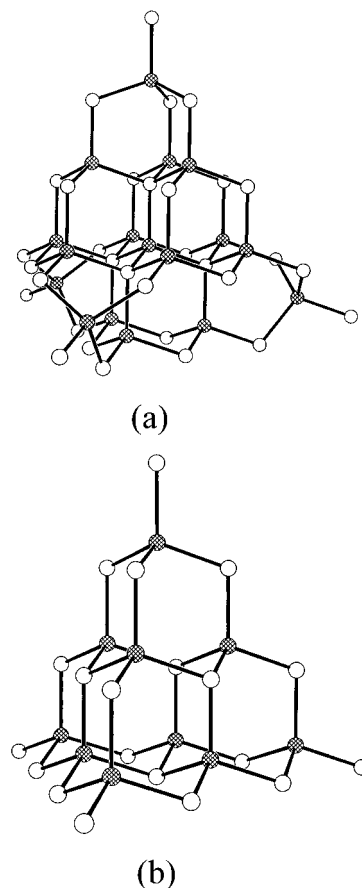


Figure 1. Structures of (a) the $\text{Cd}_{17}\text{S}_{32}$ skeleton of $[\text{S}_4\text{Cd}_{17}(\text{SPh})_{28}]^{2-}$ and (b) the $\text{Cd}_{10}\text{S}_{20}$ skeleton of $[\text{S}_4\text{Cd}_{10}(\text{SPh})_{16}]^{4-}$. Shaded atoms are Cd; unshaded atoms with one or two bonds are the S atoms of terminal or doubly bridging thiolate respectively; unshaded atoms with three or four bonds are nonthiolate S atoms.

spectroscopy.^{35–37} We investigate the reaction of the $[\text{S}_4\text{Cd}_{17}(\text{SPh})_{28}]^{2-}$ cluster shown in Figure 1a with a range of thiol ligands, and of the $[\text{S}_4\text{Cd}_{10}(\text{SPh})_{16}]^{4-}$ cluster shown in Figure 1b with ligands whose solubility properties precluded studies with $[\text{S}_4\text{Cd}_{17}(\text{SPh})_{28}]^{2-}$. We chose a reasonably wide range of thiols which were readily available, some of which also contained other functional groups that might possibly allow further functionalization of the cluster or incorporation into solid-state matrixes.

Experimental Section

Materials. The clusters $[\text{S}_4\text{Cd}_{17}(\text{SPh})_{28}](\text{Me}_4\text{N})_2$ and $[\text{S}_4\text{Cd}_{10}(\text{SPh})_{16}](\text{Me}_4\text{N})_4$ were prepared by the literature methods.^{24,25} The recrystallized $[\text{S}_4\text{Cd}_{17}(\text{SPh})_{28}](\text{Me}_4\text{N})_2$ material contained Cl impurities and consisted of a mixture of $[\text{S}_4\text{Cd}_{17}(\text{SPh})_{28}](\text{Me}_4\text{N})_2$, $[\text{S}_4\text{Cd}_{17}\text{Cl}(\text{SPh})_{27}](\text{Me}_4\text{N})_2$, and $[\text{S}_4\text{Cd}_{17}\text{Cl}_2(\text{SPh})_{26}](\text{Me}_4\text{N})_2$ in the ratios 100:31:3, as determined from the relative intensities of the corresponding peaks in the electrospray mass spectrum, [Figure 2]. The Cl^- ions originate from $(\text{Me}_4\text{N})\text{Cl}$ used in the preparation as the source of the Me_4N^+ counterions. Found: C 40.03; H 3.24; N 0.94%. Calculated for $[\text{S}_4\text{Cd}_{17}(\text{SPh})_{28}](\text{Me}_4\text{N})_2$: C 40.31; H 3.15; N 0.53%. Calculated for $[\text{S}_4\text{Cd}_{17}(\text{SPh})_{27.75}\text{Cl}_{0.25}](\text{Me}_4\text{N})_2$: C 40.11; H 3.14; N 0.54%.

(35) Colton, R.; Harrison, K. L.; Mah, Y. A.; Traeger, J. C. *Inorg. Chim. Acta* **1995**, *231*, 65–71.

(36) Colton, R.; James, B. D.; Potter, I. D.; Traeger, J. C. *Inorg. Chem.* **1993**, *32*, 2626–2629.

(37) Colton, R.; Dakternieks, D. *Inorg. Chim. Acta* **1993**, *208*, 173–177.

(24) Dance, I. G.; Choy, A.; Scudder, M. L. *J. Am. Chem. Soc.* **1984**, *106*, 6285–6295.

(25) Lee, G. S. H.; Craig, D. C.; Ma, I.; Scudder, M. L.; Bailey, T. D.; Dance, I. G. *J. Am. Chem. Soc.* **1988**, *110*, 4863–4864. Lee, G. S. H. Ph.D. Thesis, University of New South Wales, Australia, 1993.

(26) Vossmeier, T.; Reck, G.; Katsikas, L.; Haupt, E. T. K.; Schulz, B.; Weller, H. *Science* **1995**, *267*, 1476–1479.

(27) Murray, C. B.; Kagan, C. R.; Bawendi, M. G. *Science* **1995**, *270*, 1335–1338.

(28) Noglik, H.; Pietro, W. J. *Chem. Mater.* **1995**, *7*, 1333–1336.

(29) Liz-Marzán, L. M.; Giersig, M.; Mulvaney, P. *Langmuir* **1996**, *12*, 4329–4335.

(30) Bradley, D. C.; Mehrotra, R. C.; Gaur, P. D. In *Metal Alkoxides*; Academic Press: London, 1978.

(31) Løver, T.; Bowmaker, G. A.; Henderson, W.; Cooney, R. P. *Chem. Commun.* **1996**, 683–685.

(32) Løver, T.; Henderson, W.; Bowmaker, G. A.; Seakins, J. M.; Cooney, R. P. *Inorg. Chem.* **1997**, *36*, 3711.

(33) Fenn, J. B.; Mann, M.; Meng, C. K.; Wong, S. F.; Whitehouse, C. M. *Mass Spectrom. Rev.* **1990**, *9*, 37–70.

(34) Kebarle, P.; Tang, L. *Anal. Chem.* **1993**, *65*, 972A–986A.

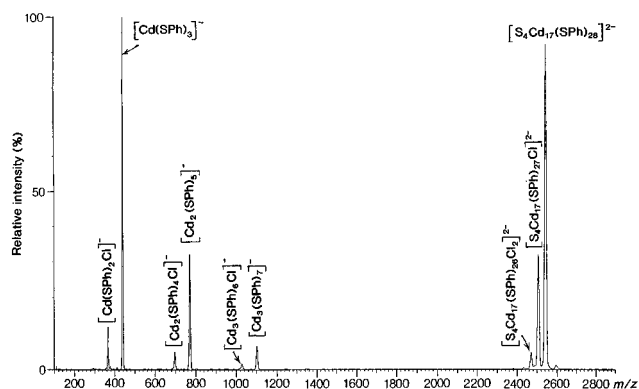


Figure 2. ES mass spectrum of $[S_4Cd_{17}(SPh)_{28}](Me_4N)_2$ at a cone voltage of 90 V. The observation of $[S_4Cd_{17}Cl(SPh)_{27}]^{2-}$ and $[S_4Cd_{17}Cl_2(SPh)_{26}]^{2-}$ shows that Cl^- (added as $(Me_4N)Cl$ to the reaction mixture during synthesis) occurs as a ligand species in the cluster. The species in the m/z region 336–1101 are fragment ions which are absent in spectra taken at cone voltages below ca. 30 V.

Ligands. *p*-Toluenethiol [$p\text{-CH}_3\text{C}_6\text{H}_4\text{SH}$], *o*-toluenethiol [$o\text{-CH}_3\text{C}_6\text{H}_4\text{SH}$], 1-dodecanethiol [$\text{CH}_3(\text{CH}_2)_{11}\text{SH}$], 2-mercaptopropionic acid [$\text{CH}_3\text{CH}(\text{SH})\text{COOH}$], 2-mercaptobenzoic acid [$o\text{-HSC}_6\text{H}_4\text{COOH}$], thioacetic acid [CH_3COSH], thiobenzoic acid [$\text{C}_6\text{H}_5\text{COSH}$], mercaptosuccinic acid [$\text{HO}_2\text{CCH}_2\text{CH}(\text{SH})\text{COOH}$], 2-mercaptoethanol [$\text{HOCH}_2\text{CH}_2\text{SH}$], 4-hydroxybenzenethiol [$\text{HOC}_6\text{H}_4\text{SH}$], 1,4- and 1,2-benzenedimethanethiol [$\text{C}_6\text{H}_4(\text{CH}_2\text{SH})_2$], 3-mercaptopropyltrimethoxysilane [$\text{HS}(\text{CH}_2)_3\text{Si}(\text{OCH}_3)_3$], sodium diethyldithiocarbamate [$\text{Et}_2\text{NCSS}^-\text{Na}^+$], potassium isopropylxanthate [$(\text{CH}_3)_2\text{CHOCS}^-\text{K}^+$], DL-cysteine [$\text{HSC}_2\text{CH}(\text{NH}_2)\text{COOH}$], 2-mercapto-5-nitrobenzimidazole [$\text{NO}_2\text{C}_6\text{H}_3\text{NHCNCSH}$], and 2-amino-4-chlorobenzenethiol hydrochloride [$\text{HSC}_6\text{H}_3(\text{NH}_2)\text{Cl}\cdot\text{HCl}$] were purchased from Aldrich and used as received.

Preparation of Reaction Mixtures. Reaction mixtures of $[S_4Cd_{17}(SPh)_{28}]^{2-}$ and the exchange ligands were prepared by dissolving the cluster in acetonitrile (HPLC grade) followed by addition of the ligand. The cluster concentration in the reaction mixture was of approximate concentration 0.1 mmol L^{-1} . The ligand-to-cluster ratio $[\text{L}]/[S_4Cd_{17}(SPh)_{28}]^{2-}$ was varied in the range from 1:1 to an excess of the ligand in order to investigate the exchange states. The solubility of the ligand in the mobile phase was a critical factor in determining whether the exchange reaction took place. The spectra were observed as soon as possible after mixing the reactants (ca. 5 min), and in general no further exchange was observed upon leaving the reaction mixtures to stand for a longer period.

Electrospray Mass Spectra (ESMS). Mass spectra were obtained in negative-ion mode using a VG Platform II mass spectrometer. Acetonitrile of HPLC grade was used as the mobile phase solvent. The spectrometer employed a quadrupole mass filter with an m/z range of 0–3000. Spectra were recorded on the freshly prepared reaction mixtures. The solution was injected into the spectrometer via a Rheodyne injector fitted with a 10 μL sample loop. A Thermo Separation Products SpectraSystem P1000 LC pump delivered the solution to the mass spectrometer source (60 $^\circ\text{C}$) at a flow rate of 0.01 mL min^{-1} , and nitrogen was employed as both the drying and the nebulizing gas. The cone voltage used was generally 30 V for $[S_4Cd_{17}(SPh)_{28}]^{2-}$ and 10 V for $[S_4Cd_{10}(SPh)_{16}]^{4-}$. These voltages gave maximum signal-to-noise ratio for the cluster ion peaks, with no or minimal fragmentation. Cone voltages were varied from 10 to 90 V in order to investigate the effect of the cone voltage on the predominant species observed. All assigned peaks in the ES mass spectra were identified by the most intense m/z value within the isotopic mass distribution. Confirmation of species was aided by comparison of the observed and predicted isotope distribution patterns. Theoretical isotope distribution patterns were calculated using the Isotope computer program.³⁸ In all cases

the agreement between the experimental and calculated isotopic distribution was excellent.

Results and Discussion

The $[S_4Cd_{17}(SPh)_{28}](Me_4N)_2$ cluster compound was chosen as the model cluster for this study. The crystalline solid consists of $[S_4Cd_{17}(SPh)_{28}]^{2-}$ anion clusters with charge-balancing $(Me_4N)^+$ cations.²⁵ The cluster $[S_4Cd_{17}(SPh)_{28}]^{2-}$ has a core with four-coordinate sulfides as in bulk CdS [Figure 1a]. Each of the four quadruply bridging S^{2-} ions is connected to a central cadmium atom, and three cadmium atoms each with tetrahedral $(\mu_4\text{-S})(\mu_2\text{-SPh})_3$ coordination. At the corners of the cluster are four cadmium atoms each with tetrahedral $(\mu_2\text{-SPh})_3(\text{SPh})$ coordination. The SPh^- ligands occur as two types: four terminal at the cluster corners and 24 doubly bridging at the edges. The solubility in acetonitrile, which is a good mobile phase solvent for ESMS, is sufficient to yield high-quality spectra. The $[S_4Cd_{17}(SPh)_{28}]^{2-}$ ion has a low charge density owing to its large size and moderately low charge. This leads to no fragmentation of the cluster at low cone voltages (<30 V). Hence the $[S_4Cd_{17}(SPh)_{28}]^{2-}$ cluster is ideally suited for ligand-exchange studies as the reaction products can be detected without interference from peaks due to fragment ions. The m/z value of 2548 is well within the 3000 m/z limit of the instrument, which allows detection of cluster species generated from exchange with ligands heavier than SPh^- (109 g mol^{-1}). The smaller $[S_4Cd_{10}(SPh)_{16}](Me_4N)_4$ cluster²⁴ [Figure 1b] has a greater solubility in acetonitrile–water mixtures compared with that of $[S_4Cd_{17}(SPh)_{28}](Me_4N)_2$. This cluster was used for mixtures containing ligands that are not sufficiently soluble in acetonitrile but are water-soluble. Experiments with $[S_4Cd_{10}(SPh)_{16}](Me_4N)_4$ were carried out under similar conditions, but with a mobile phase of 1:1 acetonitrile–water.

The full ESMS spectrum of $[S_4Cd_{17}(SPh)_{28}](Me_4N)_2$ at a cone voltage of 90 V is shown in Figure 2. The cluster ion $[S_4Cd_{17}(SPh)_{28}]^{2-}$ detected at m/z 2548 is the dominant species. The isotopic mass distribution for the peak showed the appearance of peaks at half-integral mass units. This is the signature of a doubly charged species, since the isotopes of the elements concerned (Cd, S, C) differ in mass by one mass unit. The two less intense peaks at lower m/z values are due to $[S_4Cd_{17}Cl(SPh)_{27}]^{2-}$ and $[S_4Cd_{17}Cl_2(SPh)_{26}]^{2-}$ containing an impurity of one and two Cl^- ligands, respectively. The Cl^- ions originate from $(Me_4N)Cl$ used as the source of the Me_4N^+ counterions in the preparation of the cluster. An earlier study has shown that halide ions in this system only act as terminal ligands.³² Thus, these cap at the four terminal cadmium atoms at the corner of the cluster, refer to Figure 1a. The ligands at these sites exchange the most readily. Consequently, cluster species containing chloride were not detected after reaction with ligands showing significant exchange. Fragmentation of the $[S_4Cd_{17}(SPh)_{28}]^{2-}$ ion occurs mainly by loss of $[\text{Cd}(\text{SPh})_3]^-$ species (m/z 440) and only at cone voltages higher than 40 V.³² Ligand exchange took place rapidly, and equilibrium was generally established within ca. 5 min. The dominant exchange species detected in the ES mass spectra of $[S_4Cd_{17}(SPh)_{28}](Me_4N)_2$ reacted with the different thiol ligands are

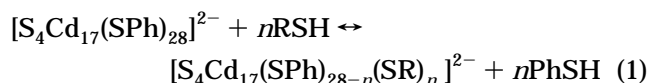
Table 1. Dominant Anionic Exchange Species Observed in the ES Mass Spectra (Cone Voltage 30 V) of $[S_4Cd_{17}(SPh)_{28}](Me_4N)_2$ Reacted with Various Thiol Ligands

compound	formula	dominant exchange species	max. no. of SPh exchanged
Alkane and Arene Thiols			
<i>p</i> -toluenethiol	CH ₃ C ₆ H ₄ SH	$[S_4Cd_{17}(SPh)_{28-n}(STol)_n]^{2-}$	28
<i>o</i> -toluenethiol	CH ₃ C ₆ H ₄ SH	$[S_4Cd_{17}(SPh)_{28-n}(STol)_n]^{2-}$	18
1-dodecanethiol	CH ₃ (CH ₂) ₁₁ SH	$[S_4Cd_{17}(SPh)_{28-n}(S(CH_2)_{11}CH_3)_n]^{2-}$	14
Dithiols			
1,4-benzenedimethanethiol	C ₆ H ₄ (CH ₂ SH) ₂	$[S_4Cd_{17}(SPh)_{28-n}(C_6H_4(CH_2SH)CH_2S)_n]^{2-}$	15 ^a
1,2-benzenedimethanethiol	C ₆ H ₄ (CH ₂ SH) ₂	$[S_4Cd_{17}(SPh)_{28-2n}(C_6H_4(CH_2S)_2)_n]^{2-}$	28
1,2-benzenedithiol	C ₆ H ₄ (SH) ₂	$[S_4Cd_{17}(SPh)_{28-2n}(C_6H_4S_2)_n]^{2-}$	24
Thiol Acids and Thio Acids			
2-mercaptopropionic acid	CH ₃ CH(SH)COOH	$[S_4Cd_{17}(SPh)_{27-2n}(CH_3CH(S)COO)_n(CH_3CH(S)COO)]^{3-}$	8 ^b
2-mercaptobenzoic acid	HSC ₆ H ₄ COOH	$[S_4Cd_{17}(SPh)_{27-2n}(SC_6H_4COO)_n(SC_6H_4COO)]^{3-}$	28 ^b
thioacetic acid	CH ₃ COSH	$[S_4Cd_{17}(SPh)_{28-n}(CH_3COS)_n]^{2-}$	9
thiobenzoic acid	C ₆ H ₄ COSH	$[S_4Cd_{17}(SPh)_{28-n}(C_6H_5COS)_n]^{2-}$	4
Thiol alcohols			
2-mercaptoethanol	HOCH ₂ CH ₂ SH	$[S_4Cd_{17}(SPh)_{28-n}(SCH_2CH_2OH)_n]^{2-}$	20
4-hydroxybenzenethiol	HO(C ₆ H ₄)SH	$[S_4Cd_{17}(SPh)_{28-n}(SC_6H_4OH)_n]^{2-}$	25
Others			
(3-mercaptopropyl)trimethoxysilane	HS(CH ₂) ₃ Si(OCH ₃) ₃	$[S_4Cd_{17}(SPh)_{28-n}\{S(CH_2)_3Si(OCH_3)_3\}_n]^{2-}$	11 ^b
DL-cysteine	HSCH ₂ CH ₂ CH(NH ₂)CO ₂ H	$[S_4Cd_{10}(SPh)_{16-2n}(SCH_2CH(NH_2)COOH)_n]^{4-}$	4
2-mercapto-5-nitrobenzimidazole	NO ₂ C ₆ H ₃ NHCNCSH	$[S_4Cd_{17}(SPh)_{28-n}(NO_2C_6H_3NHCNCS)_n]^{2-}$	5
diethyldithiocarbamate	[Et ₂ NCSS] ⁻	$[Cd(SPh)_2(Et_2NCS_2)]^-$ $[Cd(SPh)(Et_2NCS_2)_2]^-$	
isopropylxanthate	[(CH ₃) ₂ CHOCSS] ⁻	$[Cd(SPh)_2((CH_3)_2CHOCSS)]^-$ $[Cd(SPh)\{(CH_3)_2CHOCSS\}_2]^-$	
2-amino-4-chlorobenzenethiol HCl	HSC ₆ H ₃ (NH ₂)Cl	$[S_4Cd_{17}(SPh)_{28-n}(SC_6H_3(NH_2)Cl)_n]^{2-}$	6

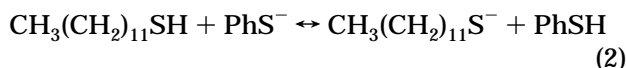
^a Due to the maximum *m/z* range of 3000 of the instrument, exchange species with higher *m/z* values could not be detected. ^b Different cluster ions were abundant at different cone voltages, see text.

given in Table 1. In most cases, only partial exchange of the thiophenolate ligands was observed. The last column in Table 1 gives the maximum number of SPh⁻ ligands exchanged, as deduced from the distribution of exchange species. This number is a measure of the extent of the exchange process, and is thus an approximate measure of the ability of the ligand concerned to cap and functionalize the cluster surface.

Alkane- and Arene Thiols Containing No Additional Functional Group. (a) *1-Dodecanethiol* [HS(CH₂)₁₁CH₃]. Exchange of SPh⁻ with [S(CH₂)₁₁CH₃]⁻ results in the detection of the ions $[S_4Cd_{17}(SPh)_{28-n}(S(CH_2)_{11}CH_3)_n]^{2-}$ in accordance with



The *m/z* range 0–3000 did not allow the detection of species heavier than the $[S_4Cd_{17}(SPh)_{19}(S(CH_2)_{11}CH_3)_9]^{2-}$ ion with a *m/z* value of 2963 [Figure 3]. However, on the basis of the distribution of observed peaks, it is expected that species up to $[S_4Cd_{17}(SPh)_{14}(SR)_{14}]^{2-}$ would be detected with a wider *m/z* range instrument. An excess of 1-dodecanethiol did not shift the peaks outside the 3000 *m/z* limit, showing that the equilibrium exchange state was biased toward capping with the thiophenolate ions. A possible reason for this is the lower acidity of 1-dodecanethiol compared with HSPH. This means that the equilibrium



lies to the left, limiting the deprotonation of 1-dodecanethiol. Steric effects are also likely to disfavor 1-dodecanethiol. As the number of 1-dodecanethiolate ligands on the cluster surface increases, the long alkyl tails of these ligands would make it increasingly difficult

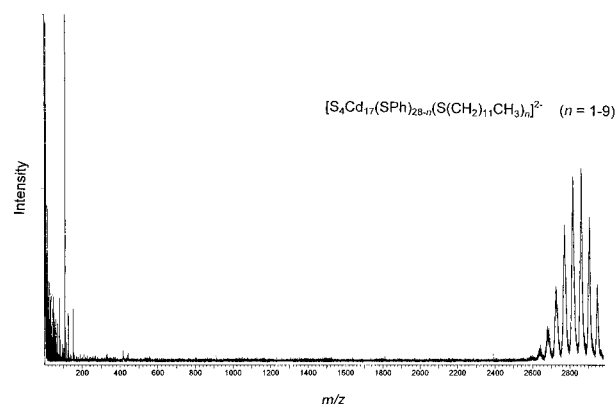


Figure 3. ES mass spectrum of a reaction mixture of $[S_4Cd_{17}(SPh)_{28}](Me_4N)_2$ and 1-dodecanethiol [HS(CH₂)₁₁CH₃] showing peaks due to the exchange ions $[S_4Cd_{17}(SPh)_{28-n}(S(CH_2)_{11}CH_3)_n]^{2-}$ (*n* = 1–9). The *m/z* range of 0–3000 did not allow the detection of heavier species than the $[S_4Cd_{17}(SPh)_{19}(S(CH_2)_{11}CH_3)_9]^{2-}$ ion with a *m/z* value of 2963.

for additional 1-dodecanthiolate ligands to bind. This view is supported by the observation that the shorter chain compound 2-mercaptoethanol shows a greater degree of exchange than does 1-dodecanethiol (Table 1; see further discussion below).

(b) *p*-Toluenethiol and *o*-Toluenethiol [CH₃C₆H₄SH]. The mass spectrum of a freshly prepared mixture of $[S_4Cd_{17}(SPh)_{28}]^{2-}$ and *p*-toluenethiol showed a shift of the *m/z* 2548 peak of $[S_4Cd_{17}(SPh)_{28}]^{2-}$ to higher *m/z* values consistent with $[S_4Cd_{17}(SPh)_{28-n}(STol)_n]^{2-}$. The relatively small mass difference of 14 mass units between thiophenolate (109) and *p*-toluenethiolate (124) gave a separation between peaks of individual cluster species of only 7 *m/z* units. This resulted in a broad envelope of unresolved peaks. The peak position of the most dominant species showed a gradual shift toward higher *m/z* values over a period of a few minutes after mixing, indicating that the equilibrium distribution of

species was not reached instantly after mixing. On addition of an excess of *p*-toluenethiol this peak was centered at (*m/z* 2735), corresponding to the ion $[\text{S}_4\text{Cd}_{17}(\text{SPh})_2(\text{STol})_{26}]^{2-}$ (*m/z* = 2737). The distribution of exchanged species appeared to fit a normal distribution curve, suggesting a random exchange process. This observation is in accord with the expectation that the methyl group should have little effect on the electronic structure of the thiol sulfur atom and its ability to bind with Cd^{2+} and that any steric effect of the methyl group in the para position would be minimal. In contrast, the exchange with *o*-toluenethiol under similar conditions appeared to be restricted, since the dominant cluster species was $[\text{S}_4\text{Cd}_{17}(\text{SPh})_{14}(\text{STol})_{14}]^{2-}$ (*m/z* 2646). The high *m/z* side of the peak envelope reached baseline level at *m/z* 2672 corresponding to $[\text{S}_4\text{Cd}_{17}(\text{SPh})_{10}(\text{STol})_{18}]^{2-}$ (*m/z* 2674), this thus being the highest exchange state observed. This situation was unchanged on aging of the solution for 5 h. By comparison, the highest exchange state observed under similar conditions with *p*-toluenethiol was $[\text{S}_4\text{Cd}_{17}(\text{STol})_{28}]^{2-}$. Steric hindrance due to the methyl group in the ortho position seems a likely explanation for the lower extent of exchange observed with *o*-toluenethiol.

At high ligand to cluster ratios, peaks were observed due to the cadmium–thiophenolate species $[\text{Cd}(\text{SPh})_{3-n}(\text{STol})_n]^-$ ($n = 0-3$), formed from the cadmium-rich $[\text{S}_4\text{Cd}_{17}(\text{SPh})_{28-n}(\text{STol})_n]^{2-}$ cluster by loss of cadmium atoms. The observation of the $[\text{Cd}(\text{SPh})_{3-n}(\text{STol})_n]^-$ ions is in accord with the fact that $[\text{Cd}(\text{SPh})_3]^-$ is the dominant fragment ion observed in the high cone voltage spectrum of $[\text{S}_4\text{Cd}_{17}(\text{SPh})_{28}]^{2-}$; refer to Figure 2.³² The cadmium atoms that are most readily removed are presumably the four terminal cadmium atoms at the corners of the cluster. The stripping of cadmium atoms from the cluster surface results in the observation of peaks due to mixed-ligand species of the smaller $[\text{S}_4\text{Cd}_{10}(\text{SPh})_{16-n}(\text{STol})_n]^{4-}$ cluster in the *m/z* range 750–806. Hence, in the presence of an excess of thiol, the cadmium-rich cluster loses a total of seven cadmium atoms to $[\text{Cd}(\text{SPh})_{3-n}(\text{SR})_n]^-$ ions and converts to $[\text{S}_4\text{Cd}_{10}(\text{SPh})_{16-n}(\text{SR})_n]^{4-}$. No intermediate cluster species were observed. The cluster transformation involves rearrangement of the sulfur atoms of the core from being four-coordinate to three-coordinate. In all cases when a ligand showing significant exchange was added in excess, the formation of $[\text{Cd}(\text{SPh})_{3-n}(\text{SR})_n]^-$ fragment ions and transformation to the $[\text{S}_4\text{Cd}_{10}(\text{SPh})_{16-n}(\text{SR})_n]^{4-}$ cluster occurred. A strong peak due to the thiolate anions SR^- was also observed in each case.

From the study of the exchange behavior of *o*- and *p*-toluenethiol and 1-dodecanethiol it is evident that the $[\text{S}_4\text{Cd}_{17}(\text{SPh})_{28}]^{2-}$ cluster effectively reveals differences in ligand behavior. Further examples of this are observed in the systems discussed below.

Thiol Acids $[\text{R}(\text{SH})\text{COOH}]$ and Thio Acids $[\text{RCOSH}]$. The thiol acids are interesting bifunctional ligands because of the affinity of the carboxylic acid group for metals, including the transition metals.³⁰ For example, when the metal alkoxides $\text{M}(\text{OR})_4$ ($\text{M} = \text{Ti}, \text{Zr}$) are reacted with carboxylic acids, some of the alkoxide groups are substituted by carboxylate groups. The potential of binding these modified metal alkoxides to the surface of CdS clusters opens up interesting opportunities for preparing new hybrid materials such

as layered nanoclusters of CdS/MO_2 . Combining a small bandgap semiconductor with a large bandgap semiconductor offers opportunities to sensitize the latter, which may find applications in photocatalysis, solar energy conversion, etc. Nanoparticles of TiO_2 have recently been coupled to nanoparticles of PbS and CdS through the carboxylic end of mercaptocarboxylic acids $\text{HS}-(\text{CH}_2)_n-\text{COOH}$ ($n = 1-3$).^{39,40}

(a) *2-Mercaptopropionic Acid* $[\text{CH}_3\text{CH}(\text{SH})\text{COOH}]$. The 30 V spectrum of a reaction mixture of $[\text{S}_4\text{Cd}_{17}(\text{SPh})_{28}]^{2-}$ and 2-mercaptopropionic acid was dominated by peaks in the *m/z* range 1390–1659 separated by 38 *m/z* units in addition to the *m/z* 2548 peak of $[\text{S}_4\text{Cd}_{17}(\text{SPh})_{28}]^{2-}$ [Figure 4a]. Notably, the exchange did not involve $[\text{CH}_3\text{CH}(\text{S})\text{COOH}]^-$ ions. The difference of four mass units between $[\text{CH}_3\text{CH}(\text{S})\text{COOH}]^-$ (105 g mol⁻¹) and SPh^- (109 g mol⁻¹) would have caused an observable broadening and a small downward shift in the *m/z* 2548 peak of $[\text{S}_4\text{Cd}_{17}(\text{SPh})_{28}]^{2-}$ if significant exchange with $[\text{CH}_3\text{CH}(\text{S})\text{COOH}]^-$ ions had occurred. The isotopic mass distribution of the dominant species showed peaks separated by *m/z* 0.33, characteristic of triply charged ions. The peak separation of 38 *m/z* units therefore corresponds to a difference of 114 mass units. This is in excellent agreement with the mass difference between two SPh^- ligands and one doubly charged $[\text{CH}_3\text{CH}(\text{S})\text{COO}]^{2-}$ ligand. This shows that each dianion $[\text{CH}_3\text{CH}(\text{S})\text{COO}]^{2-}$ replaces two SPh^- ligands by chelating to neighboring cadmium atoms at the cluster surface through the thiol group and one of the oxygen atoms of the carboxylic acid group. The above exchange scheme does not account for the fact that the ions are triply charged, i.e., have acquired one extra negative charge compared with $[\text{S}_4\text{Cd}_{17}(\text{SPh})_{28}]^{2-}$. This most likely occurs through loss of an H^+ from a $[\text{CH}_3\text{CH}(\text{S})\text{COOH}]^-$ ligand bonded terminally to one of the four Cd atoms at the corner of the cluster. Thus the observed ions are $[\text{S}_4\text{Cd}_{17}(\text{SPh})_{27-2n}(\text{CH}_3\text{CH}(\text{S})\text{COO})_n(\text{CH}_3\text{CH}(\text{S})\text{COO})^t]^{3-}$ ($n = 1-8$), where *c* and *t* stand for chelating and terminal, respectively. Similarly, the 4⁻, 5⁻, and 6⁻ clusters would be expected to form by further loss of protons from terminal $[\text{CH}_3\text{CH}(\text{S})\text{COOH}]^-$ ligands at the other three corners. Consistent with this was the occurrence of a new envelope of peaks in the region *m/z* = 1072–1243 calculated for the 4⁻ ions upon lowering the cone voltage to 10 V [Figure 4b]. The detection of these ions only at low cone voltages is due to the higher charge, which results in lower stability. The even more highly charged 5⁻ and 6⁻ species were not detected. The 3⁻ ions, dominant at 30 V, nearly disappeared from the spectrum when the cone voltage was increased to 45 V and were replaced with the 2⁻ ions $[\text{S}_4\text{Cd}_{17}(\text{SPh})_{28-2n}(\text{CH}_3\text{CH}(\text{S})\text{COO})_n]^{2-}$ [Figure 4c]. Again, this is in accord with the fact that species with a lower charge density are more stable at higher voltages.

(b) *2-Mercaptobenzoic Acid* $[\text{HSC}_6\text{H}_4\text{COOH}]$. 2-Mercaptobenzoic acid behaved similarly to 2-mercaptopropionic acid. The triply charged ions $[\text{S}_4\text{Cd}_{17}(\text{SPh})_{27-2n}(\text{SC}_6\text{H}_4\text{COO})_n(\text{SC}_6\text{H}_4\text{COO})^t]^{3-}$ ($n = 1-13$) were abundant at 10 V. The ion $[\text{S}_4\text{Cd}_{17}(\text{SPh})_{23}(\text{SC}_6\text{H}_4\text{COO})_2(\text{SC}_6\text{H}_4\text{COO})^t]^{3-}$ ($n = 2$) at *m/z* 1669 was

(39) Sun, Y.; Hao, E.; Zhang, X.; Yang, B.; Gao, M.; Shen, J. *Chem. Commun.* **1996**, 2381–2382.

(40) Lawless, D.; Kapoor, S.; Meisel, D. *J. Phys. Chem.* **1995**, *99*, 10329–10335.

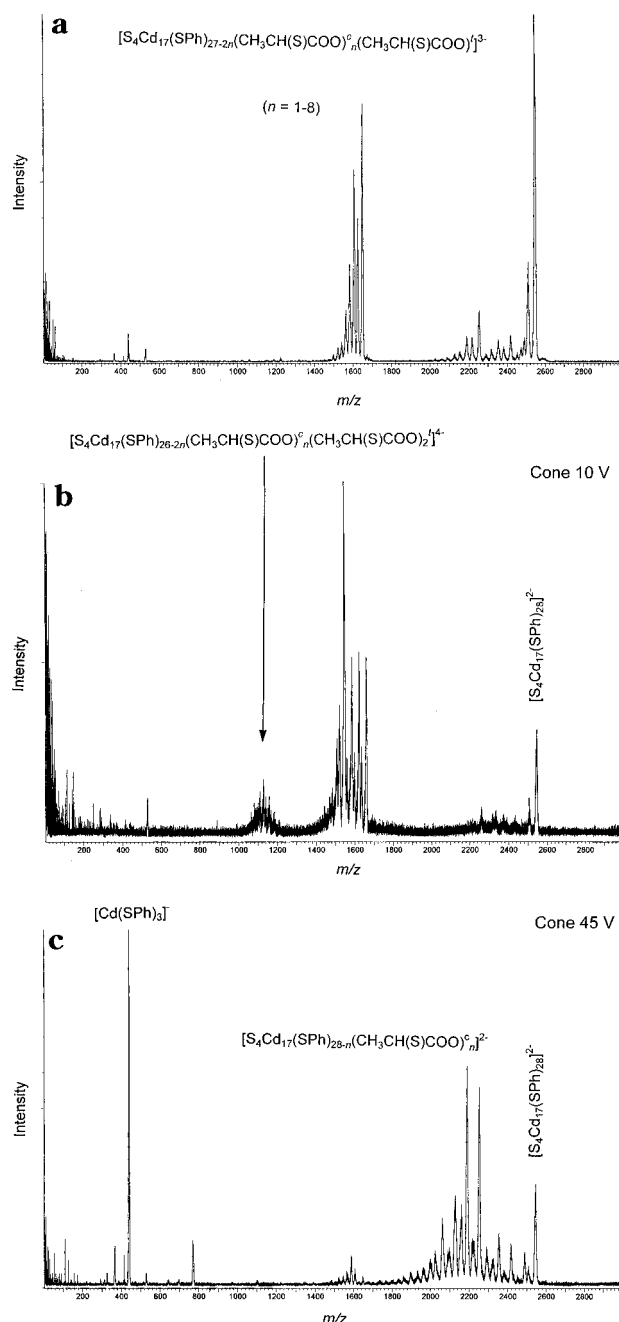


Figure 4. ES mass spectra of a reaction mixture of $[S_4Cd_{17}(SPh)_{28}](Me_4N)_2$ and 2-mercaptopropionic acid. The 30 V spectrum (a) shows dominant peaks due to $[S_4Cd_{17}(SPh)_{27-2n}(CH_3CH(S)COO)_c^n(CH_3CH(S)COO)_t]^{3-}$ ($n = 1-8$) in addition to the m/z 2548 peak of $[S_4Cd_{17}(SPh)_{28}]^{2-}$ (c stands for chelating ligand and t for terminal bound ligand). The 10 V spectrum (b) show additional peaks in the region $m/z = 1070-1240$ due to the 4^- ions $[S_4Cd_{17}(SPh)_{26-2n}(CH_3CH(S)COO)_c^n(CH_3CH(S)COO)_t]^{4-}$ which, owing to their high charge, are only stable at low cone voltages. The 2^- ions $[S_4Cd_{17}(SPh)_{28-2n}(CH_3CH(S)COO)_c^n]^{2-}$ dominate the 45 V spectrum (c), because the low charge density make these species more stable at high cone voltages.

the most abundant, with decreasing relative abundances for the more highly exchanged clusters. The $n = 1$ ion $[S_4Cd_{17}(SPh)_{25}(SC_6H_4COO)_c(SC_6H_4COO)_t]^{3-}$ at m/z 1691 was observed only at low concentrations of 2-mercaptobenzoic acid, and the $n = 0$ case was not observed. This suggests a preference for the chelating bonding mode. The relative abundances of the more highly substituted species did not seem to increase with increasing concentration of 2-mercaptobenzoic acid.

However, among the 2^- ions that again became dominant at the higher cone voltage of 45 V, the completely exchanged ion $[S_4Cd_{17}(SC_6H_4COO)_{14}]^{2-}$ (m/z 2085) was the most abundant. The two spectra taken at 10 and 45 V therefore appear to reveal different distributions of species. The unsymmetrical distribution of peaks in the 10 V spectrum (similar to that observed in the 30 V spectrum of 2-mercaptopropionic acid in Figure 4a) showed increasingly lower intensities of the peaks corresponding to the more highly substituted species. This may be explained by the nature of the ionization process leading to these 3^- ions. With increasing surface coverage of chelating $[SC_6H_4COO]^{2-}$ ligands, the existence of the less favored terminally bound $[SC_6H_4COOH]^-$ species, which can lose a proton, becomes increasingly less probable.

(c) *Thioacetic Acid* $[CH_3COSH]$ and *Thiobenzoic Acid* $[C_6H_5COSH]$. We now compare the results for 2-mercaptopropionic acid and 2-mercaptobenzoic acid with those of thioacetic acid $[CH_3COSH]$ and thiobenzoic acid $[C_6H_5COSH]$. The reaction with thioacetic acid $[CH_3COSH]$ gave the doubly charged exchange species $[S_4Cd_{17}(SPh)_{28-n}(CH_3COS)_n]^{2-}$ ($n = 1-9$), resulting from simple exchange of SPh^- with $[CH_3COS]^-$. By comparison with thioacetic acid, thiobenzoic acid $[C_6H_5COSH]$ appeared more restricted in its exchange ability and gave $[S_4Cd_{17}(SPh)_{24}(C_6H_5COS)_4]^{2-}$ as the highest exchange state with an excess of thiobenzoic acid. In both cases, strong peaks due to the fragment species $[Cd(RCOS)_3]^-$ at m/z 338 and 524, respectively, were observed, accompanied by weak peaks due to $[Cd(SPh)_{3-n}(RCOS)_n]^-$ ($n = 1-2$). This shows that the functional group $-COS^-$ has a tendency to remove cadmium atoms from the surface of the cluster. This behavior would suggest that the ability of the ligands to form bridging bonds between neighboring cadmium atoms is limited, and in this case a preference for $-COS^-$ to chelate via the oxygen and sulfur atoms, forming bonds to the same cadmium atom, seems likely. The fact that exchange of as much as nine SPh^- ligands was observed with thioacetic acid shows that some bridging of neighboring cadmium atom by $[CH_3COS]^-$ occurs. The lower extent of exchange observed for thiobenzoic acid compared with thioacetic acid suggests that thiobenzoic acid is less able to form bridging bonds. The behavior of the thio acids contrasts with that observed for the thiol acids $R(SH)COOH$ in the previous section. The latter replaced two bridging SPh^- ligands by chelating to neighboring cadmium atoms through the thiol group and one of the oxygen atoms of the carboxylic acid group. Both the sulfur and the oxygen atoms formed bridging bonds like those of the original SPh^- ligands, thereby leaving the cluster intact.

Thiol alcohols. *2-Mercaptoethanol* $[HOCH_2CH_2SH]$ and *4-Hydroxybenzenethiol* $[HOC_6H_4SH]$. Similar to the situation for the monothiocarboxylic acids described in the preceding section, thiol alcohols $[HSROH]$ contain both a hard oxygen donor site and a soft sulfur donor site which can lead to aggregation of soft and hard metal centers.

Facile exchange occurred with 2-mercaptoethanol, resulting in an envelope of peaks due to $[S_4Cd_{17}(SPh)_{28-n}(SCH_2CH_2OH)_n]^{2-}$ ($n = 1-20$) ions. No triply charged species were observed, showing that the alcohol group does not readily lose its proton. As anticipated, 4-hy-

droxybenzenethiol [$\text{HSC}_6\text{H}_4\text{OH}$] exchanges readily with thiophenolate to give $[\text{S}_4\text{Cd}_{17}(\text{SPh})_{28-n}(\text{SC}_6\text{H}_4\text{OH})_n]^{2-}$ ($n = 0-25$) ions. Also detected was a series of less abundant 3^- ions dominated by $[\text{S}_4\text{Cd}_{17}(\text{SPh})_{15}(\text{SC}_6\text{H}_4\text{OH})_{12}(\text{SC}_6\text{H}_4\text{O})]^{3-}$ (m/z 1768). This corresponds to the dominant 2^- ion, which is $[\text{S}_4\text{Cd}_{17}(\text{SPh})_{15}(\text{SC}_6\text{H}_4\text{OH})_{13}]^{2-}$ (m/z 2652). The 3^- ions originate from the 2^- ions by loss of a proton from the OH group of one of the $[\text{SC}_6\text{H}_4\text{OH}]^-$ ligands. The fact that the 3^- ions which were absent for 2-mercaptoethanol are observed in this case is consistent with a higher acidity of 4-hydroxybenzenethiol.

Dithiols. The behavior of 1,4-benzenedimethanethiol [$\text{C}_6\text{H}_4(\text{CH}_2\text{SH})_2$] is similar to that of 4-hydroxybenzenethiol [$\text{HSC}_6\text{H}_4\text{OH}$]. Facile exchange resulted in the observation of $[\text{S}_4\text{Cd}_{17}(\text{SPh})_{28-n}(\text{C}_6\text{H}_4(\text{CH}_2\text{SH})\text{CH}_2\text{S})_n]^{2-}$ [Figure 5a]. Again, the absence of more highly charged clusters showed that the second thiol group does not readily lose its proton. Also, as expected on the basis of the rigidity of the benzene ring, the second thiol group cannot bond to a cadmium ion at the surface. However, S,S-chelating by $[\text{C}_6\text{H}_4(\text{CH}_2\text{S})_2]^{2-}$ to individual Cd atoms on the cluster surface can occur for 1,2-benzenedimethanethiol. The second thiol group appearing in the ortho position facilitates this. An envelope of peaks occurred at the lower m/z side of the 2548 peak of $[\text{S}_4\text{Cd}_{17}(\text{SPh})_{28}]^{2-}$ with an m/z separation of 25 m/z units between each peak [Figure 5b]. This is consistent with the substitution of two SPh $^-$ for each bridging $[\text{C}_6\text{H}_4(\text{CH}_2\text{S})_2]^{2-}$. Accordingly, the lowest m/z peak was that of $[\text{S}_4\text{Cd}_{17}(\text{C}_6\text{H}_4(\text{CH}_2\text{S})_2)_{14}]^{2-}$ (m/z 2198) which has had all the original SPh $^-$ ligands replaced. This species became dominant when 1,2-benzenedimethanethiol was added in excess [Figure 5c]. Identical behavior was found for 1,2-benzenedithiol [$\text{C}_6\text{H}_4(\text{SH})_2$].

3-Mercaptopropyltrimethoxysilane [$\text{HS}(\text{CH}_2)_3\text{Si}(\text{OCH}_3)_3$]. Alkoxysilanes of the type $\text{RSi}(\text{OR})_3$ are widely used reagents for the functionalization of glass and oxide surfaces and in the formation of siloxane-based polymers.⁴¹ The synthesis of nanosized gold-silica layered particles has recently been achieved using (3-aminopropyl)trimethoxysilane $\text{NH}_2(\text{CH}_2)_3\text{Si}(\text{OCH}_3)_3$ as a coupler.²⁹ The amino groups bind to the gold surface by gold-amine bonds and the silanol groups $\text{Si}(\text{OH})_3$ formed by hydrolysis of the $\text{Si}(\text{OCH}_3)_3$ groups react with silicate SiO_3^{2-} with the release of water generating a silica layer, SiO_2 . By analogy with this method, the formation of a TiO_2 or ZrO_2 oxide layer should be possible by binding the alkoxides $\text{Ti}(\text{OR})_4$ and $\text{Zr}(\text{OR})_4$ instead of SiO_3^{2-} : $\text{Au}-\text{N}(\text{CH}_2)_3\text{Si}(\text{OH})_3 + \text{M}(\text{OR})_4 \rightarrow \text{Au}-\text{N}(\text{CH}_2)_3\text{Si}(\text{OH}_2)-\text{O}-\text{M}(\text{OR})_3 + \text{HOR}$ followed by hydrolysis. The use of CdS nanoclusters functionalized with thiol-silanes such as 3-(mercapto-propyl)trimethoxysilane may result in the coating of such particles with an oxide layer of TiO_2 or ZrO_2 . (3-Mercaptopropyl)trimethoxysilane [$\text{HS}(\text{CH}_2)_3\text{Si}(\text{OCH}_3)_3$] readily exchanged with SPh $^-$ to give the silane-functionalized clusters $[\text{S}_4\text{Cd}_{17}(\text{SPh})_{28-n}\{\text{S}(\text{CH}_2)_3\text{Si}(\text{OCH}_3)_3\}_n]^{2-}$ ($n = 1-11$). Figure 6a shows the spectrum at a low ligand to cluster ratio with $n = 6$ as the highest exchange state. Intensities are observed between the major peaks of $[\text{S}_4\text{Cd}_{17}(\text{SPh})_{28-n}\{\text{S}(\text{CH}_2)_3\text{Si}(\text{OCH}_3)_3\}_n]^{2-}$.

(41) Plueddman, E. D. in *Silylated Surfaces*; Leyden, D. E., Collins, W. T., Eds.; Gordon and Breach Science Publishers Inc.: New York, 1980; pp 31-53.

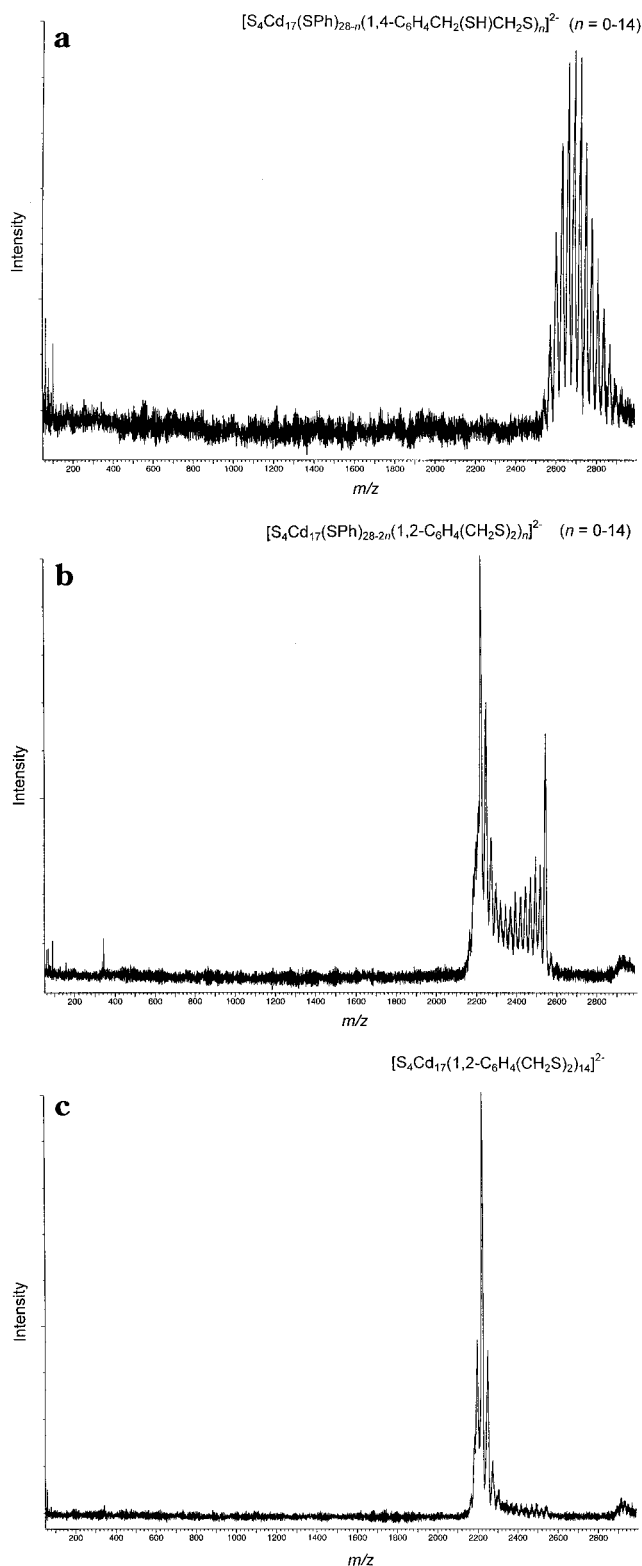


Figure 5. ES mass spectrum of $[\text{S}_4\text{Cd}_{17}(\text{SPh})_{28}]^{2-}$ after reaction with (a) 1,4- and (b) 1,2-benzenedimethanethiol [$\text{C}_6\text{H}_4(\text{CH}_2\text{SH})_2$]. The reaction with 1,4-benzenedimethanethiol involves exchange of $[\text{1,4-C}_6\text{H}_4(\text{CH}_2\text{SH})(\text{CH}_2\text{S})]^-$ giving $[\text{S}_4\text{Cd}_{17}(\text{SPh})_{28-n}(\text{1,4-C}_6\text{H}_4(\text{CH}_2\text{SH})\text{CH}_2\text{S})_n]^{2-}$, while exchange with 1,2-benzenedimethanethiol yields the $[\text{S}_4\text{Cd}_{17}(\text{SPh})_{28-2n}(\text{1,2-C}_6\text{H}_4(\text{CH}_2\text{S})_2)_n]^{2-}$ ions ($n = 1-14$) resulting from S,S-chelating by $[\text{C}_6\text{H}_4(\text{CH}_2\text{S})_2]^{2-}$ ions to individual Cd atoms on the cluster surface.

The observation of weak peaks due to the silanols $[\text{S}(\text{CH}_2)_3\text{Si}(\text{OCH}_3)_{3-m}(\text{OH})_m]$ at m/z 181, 167, and 153 suggested that the extra intensities were due to hydrolyzed silane ligands on the cluster. Hydrolysis of the

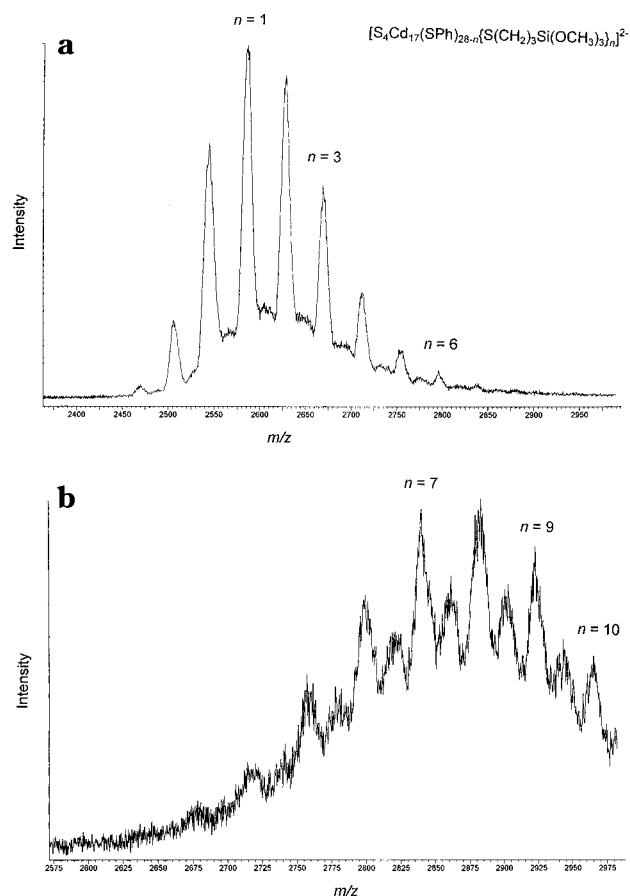


Figure 6. ES mass spectrum of $[S_4Cd_{17}(SPh)_{28}](Me_4N)_2$ reacted with small amounts of (3-mercaptopropyl)trimethoxysilane $[HS(CH_2)_3Si(OCH_3)_3]$ shows peaks due to the silane-functionalized clusters $[S_4Cd_{17}(SPh)_{28-n}\{S(CH_2)_3Si(OCH_3)_3\}_n]^{2-}$ ($n = 1-6$), spectrum (a). Hydrolysis of the $Si(OCH_3)_3$ groups to $Si(OCH_3)_{3-m}(OH)_m$ due to some water present in the solvent yields intensities between each of these major peaks. (b) The spectrum of a mixture containing an excess of (3-mercaptopropyl)trimethoxysilane and water.

$Si(OMe)_3$ groups to silanol $Si(OCH_3)_{3-m}(OH)_m$ ($m = 1-3$) is known to occur rapidly,⁴¹ and this is likely to occur if a small amount of water is present in the solvent. An additional series of peaks centered on m/z 1850 was observed. These were due to triply charged clusters and can be explained by loss of a proton from the OH groups of surface-bonded silanol ligands.

The spectrum of a mixture containing both an excess of the silane ligand and water showed stronger well-defined peaks occurring between the major peaks [Figure 6b]. These cannot be explained simply by silanol ligands. For n silane ligands on the cluster, the number of (OCH_3) groups hydrolyzed to (OH) groups is between 0 and $3n$, where $3n$ corresponds to complete hydrolysis. This would give peaks separated by 7 m/z units. The observed peaks do not agree with this, and assignments have not been found. After aging of the mixture for 12 h an insoluble precipitate formed, indicating that condensation of the silanol groups and polymerization of the clusters in a siloxane polymer had occurred. Far-infrared spectra showed that the cluster cores remain intact in this product due to capping silanethiol and SPh^- .

Diethyldithiocarbamate $[(C_2H_5)_2NCSS]^-$ and Isopropylxanthate $[(CH_3)_2CHOCS]^-$. Redox species that strongly interact with a semiconductor surface are

of great importance in improving the performance of photoelectrochemical cells. The light-energy conversion efficiency of CdX ($X = S, Se$) based electrochemical cells are enhanced by employing diethyldithiocarbamate as the redox systems.^{42,43} Colloids of CdS undergo complexation with diethyldithiocarbamate anions in two stages. Interaction of $Et_2NCS_2^-$ with the surface initially results in partial dissolution of the particles by loss of Cd from the surface, followed by surface modification with $Et_2NCS_2^-$.⁴⁴ When extremely small CdS particles are brought into contact with excess of $Et_2NCS_2^-$, complete dissolution of the particle has been reported.⁴⁴ Dithiocarbamate anions $[R_2NCSS]^-$ can act as either bridging ligands or as terminal S,S-chelating ligands. Our aim was to probe the interaction of the $Et_2NCS_2^-$ ion with the $[S_4Cd_{17}(SPh)_{28}]^{2-}$ cluster and to identify the dominant reaction species.

In a mixture of $Et_2NCS_2^-$ and $[S_4Cd_{17}(SPh)_{28}]^{2-}$ of mole ratio 4:1 no ligand-exchanged clusters were detected. However, the fragment ions $[Cd(SPh)_2(Et_2NCS_2)]^-$ (m/z 479) and $[Cd(SPh)(Et_2NCS_2)_2]^-$ (m/z 518) were abundant, showing removal of Cd^{2+} from the cluster surface. Consistent with this was the detection of a strong peak due to $[S_4Cd_{10}(SPh)_{16}]^{4-}$. By comparison, the thiols caused the transformation to $[S_4Cd_{10}(SPh)_{16}]^{4-}$ only when added in large excess. At a ratio of $[Et_2NCS_2]^-$ to $[S_4Cd_{17}(SPh)_{28}]^{2-}$ of 14:1 the spectrum contained only the peaks due to $[Cd(SPh)_2(Et_2NCS_2)]^-$ and $[Cd(SPh)(Et_2NCS_2)_2]^-$, with the latter being most abundant. At this composition a yellow powder, identified as bulk CdS by its far-IR absorption spectrum, precipitated within minutes. The formation of bulk CdS would result from aggregation of uncapped cluster cores. The isopropylxanthate ligand $[(CH_3)_2CHOCS]^-$ showed behavior similar to that of dithiocarbamate, as was expected based on the similarity in the chemical structures. The tendency for these ions to remove the surface cadmium atoms would suggest a preference for the formation of terminal S,S-chelating bonds with cadmium in this system. Similar behavior, although less marked, was observed for the thio acids (RCOSH) thioacetic acid and thiobenzoic acid (see above). This is consistent with the similarity between the $-COS^-$ and $-CSS^-$ functional groups in these ligands.

dl-Cysteine $[HSCH_2CH(NH_2)COOH]$. No exchange was observed when DL-cysteine was added to $[S_4Cd_{17}(SPh)_{28}]^{2-}$ in acetonitrile, due to poor solubility in this solvent. Exchange occurred when the cluster $[S_4Cd_{10}(SPh)_{16}]^{4-}$ in a 1:1 acetonitrile-water mobile phase was used. The species detected in the 10 V spectrum of the freshly made mixture were the clusters $[S_4Cd_{10}(SPh)_{16-n}(SCH_2CH(NH_2)COOH)_n]^{4-}$, with $n = 4$ as the highest exchange state. Also observed were peaks due to $[SCH_2CH(NH_2)COO]^{2-}$ (m/z 61), $[SCH_2CH(NH_2)COOH]^-$ (m/z 121), $[Cd(SPh)_2(SCH_2CH(NH_2)COOH)]^-$ (m/z 451), and $[Cd(SPh)(SCH_2CH(NH_2)COOH)_2]^-$ (m/z 462). As the thiophenolate surface is replaced by cysteine the solubility of the cluster is expected to decrease. This is a likely explanation.

(42) Thackeray, J. W.; Natan, M. J.; Ng, P.; Wrighton, M. S. *J Am Chem Soc* **1986**, *108*, 3570-3577.

(43) Natan, M. J.; Thackeray, J. W.; Wrighton, M. S. *J Phys Chem* **1986**, *90*, 4089-4098.

(44) Kamat, P. V.; Dimitrijević, N. M. *J Phys Chem* **1989**, *93*, 4259-4263.

tion for the absence of species containing a higher proportion of cysteine. A cloudy solution formed when the mixture was heated at 80 °C for 10 min.

2-Amino-4-chlorobenzenethiol HCl[HSC₆H₃(NH₂)Cl]. The doubly charged ions [S₄Cd₁₇(SPh)_{28-n}⁻(SC₆H₃(NH₂)Cl)_n]²⁻ (*n* = 0–6) were dominant, with the occurrence of less intense peaks due to the corresponding triply charged species [S₄Cd₁₇(SPh)_{27-n}⁻(SC₆H₃(NH₂)Cl)_n(SC₆H₃NHCl)]³⁻ formed from the doubly charged clusters by loss of a proton from the amino group of a [SC₆H₃(NH₂)Cl]⁻ ligand.

Summary and Conclusions

The capping and functionalization of the CdS nanocluster [S₄Cd₁₇(SPh)₂₈]²⁻ is conveniently studied by electrospray mass spectrometry using ligand-exchange reactions. The technique reveals the preferred binding modes of different types of thiol ligands. This yields information about the ability of a given ligand to cap and functionalize the cluster surface. The interaction of reactive species, such as the diethyldithiocarbamate ion, with the cluster can be directly monitored by observation of the dominant reaction products. The extent of exchange observed for the various ligands is sensitive to steric effects, the stability of the thiolate ion of the exchange ligand compared with the thiophenolate ion, and the solubility of the ligand in acetonitrile. The structure of the capping layer of [S₄Cd₁₇(SPh)₂₈]²⁻ is representative of thiolate-capped clusters, and the behavior of this cluster can be expected to mimic the

situation for larger thiolate-capped particles. ESMS provides the most convenient method for rapidly determining the products of such exchange reactions, since a single chemical species gives a single "band" in the spectrum, which generally does not overlap with the bands due to other chemical species present. This would not be the case for the other techniques, which produce several bands in overlapping regions (NMR, IR) or only a relatively broad band (UV-vis). Moreover, the position and structure of the ESMS band immediately gives the charge and mass of the species concerned, so that its identity can be easily established. This contrasts with the other techniques mentioned, which are more suited to the determination of the structure of species of known elemental composition, rather than to the determination of composition per se. Nevertheless, it is expected that that specific exchange species of the type identified in this study could be isolated and further characterized by other techniques such as those mentioned above.

Acknowledgment. We thank the Universities of Auckland and Waikato for financial support and the New Zealand Lottery Grants Board for a grant-in-aid toward the mass spectrometer. The support of this work from 3M through financial support and a Ph.D. scholarship to T.L. is gratefully acknowledged. We thank Wendy Jackson for technical assistance with the mass spectrometer.

CM970148Q